Selective Deficiency of HIF-1α in Myeloid Cells Influences Secondary Intention Wound Healing in Mouse Skin

RICHARD A. OWINGS[1], MARJAN BOERMA[2], JUNRU WANG[2], MAAIKE BERBEE[2],
KEITH R. LADEROUTE[3], LEE S.F. SODERBERG[4], EMRE VURAL[5,6] and MARTIN HAUER JENSEN[2,6]

Departments of [1]Pathology, [2]Pharmaceutical Sciences,
[4]Microbiology and Immunology, and
[5]Otolaryngology, University of Arkansas for Medical Sciences, Little Rock, AR;
[3]Biosciences Division, SRI International, Menlo Park, CA;
[6]Surgical Services, Central Arkansas Veterans Healthcare System, Little Rock, AR, U.S.A.

Abstract. *Background: Hypoxia-inducible factor-1 (HIF-1) influences myeloid cell function. In this study we examined the role of myeloid cell HIF-1α on wound healing in vivo using a cell-specific knockout (KO) mouse model. Materials and Methods: HIF-1α KO mice and wild-type (WT) controls received 8 mm full thickness dorsal dermal wounds. Wound dimensions were measured until full closure. Tissue was obtained from 3-day-old wounds for (immuno-)histochemical analysis. Production of interleukin-1β (IL-1β) and nitric oxide (NO) in response to lipopolysaccharide (LPS) and/or desferrioxamine (DFX) was examined in vitro. Results: Early wound closure occurred significantly faster in HIF-1α KO mice than in WT mice. Wounds of KO mice contained similar numbers of neutrophils and macrophages, but more activated keratinocytes, consistent with accelerated re-epithelialization. Interestingly, while LPS and LPS+DFX elicited a similar IL-1β response in macrophages from the 2 mouse types, NO production was blunted in HIF-1α KO macrophages. Conclusion: Absence of HIF-1α in myeloid cells accelerates the early phase of secondary intention wound healing in vivo. This may be associated with a deficient ability of myeloid cells to initiate an appropriate NO production response. Pharmacologic modulators of HIF-1α should be explored in situations with abnormal wound healing.*

Wound healing is a complex process that consists of several partially overlapping phases, including hemostasis, inflammation, proliferation, and resolution. Myeloid cells play important and well-established roles during the early phase of the wound healing response. Hence, both neutrophils and macrophages are attracted to the wound site during the inflammatory phase. Neutrophils clear microbes and cellular debris from the wounded area, but may also cause injury to normal cells by bursts of reactive oxygen and nitrogen species. During the wound healing process, macrophages phagocytize microbes, debris and damaged cells, and release a plethora of growth factors and cytokines that stimulate progression of the wound from inflammation to re-epithelization and/or scar formation (1, 2).

Recent evidence has revealed that the oxygen-sensitive transcription factor, hypoxia inducible factor-1 alpha (HIF-1α) is a critical regulator of myeloid cell function in physiological and pathological states. For example, myeloid cells that lack HIF-1α exhibit reduced glycolysis, reduced ATP levels, and reduced aggregation, invasion, and motility (3). Moreover, while the main function of HIF-1α is to regulate the expression of genes that mediate adaptation to low oxygen levels (4), HIF-1α may also be induced by other factors, such as cytokines, produced during wound healing (5).

This study used a mouse model with a myeloid cell lineage selective deficiency of HIF-1α (3) to specifically address the role of HIF-1α in the wound healing response *in vivo* and on the production of interleukin (IL)-1β and nitric oxide (NO) *in vitro*. Our findings point to HIF-1α as a potential pharmacologic target in conditions with abnormal wound healing.
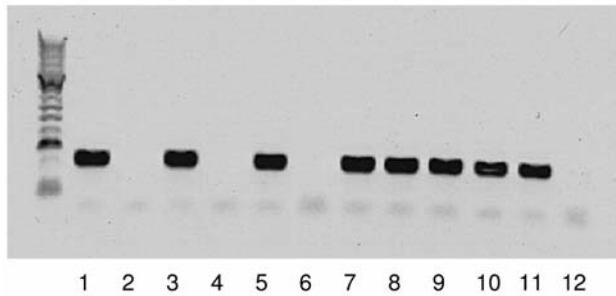
Figure 1. *Polymerase chain reaction (PCR) detection of the Cre recombinase gene. DNA was isolated from tail snips, amplified (see text), and resolved by agarose gel electrophoresis. Of the 12 samples shown, samples 1, 3, 5, and 7-11 show presence of the Cre recombinase gene.*

Materials and Methods

Mouse model. Breeders used to generate the mutant mice used in this study were on a mixed Sv129/C57Bl/6/CB.20 background and were kindly provided by Dr. R.S. Johnson, University of California at San Diego, CA, USA (3). Myeloid-selective HIF-1α KO (HIF-1α-lysMcre) mice are double mutants that carry a Cre (cyclization recombination) recombinase gene under the control of the endogenous M lysozyme promoter (6), as well as a HIF-1α gene flanked by *LoxP* (locus of X-over P1) sites ("double floxed"). The WT mice carry the double-floxed HIF-1α gene only (without Cre recombinase). Myeloid-selective expression of Cre recombinase in the presence of a double-floxed HIF-1α gene excises the gene in at least 75% of neutrophils and macrophages (3). Animals were housed under standardized conditions with controlled temperature, humidity, and a 12-12 h light-dark cycle, and had free access to chow and tap water for the duration of the study.

Each mouse used for this study was tested for the presence (KO) or absence (WT) of the Cre recombinase gene by PCR (Figure 1). Tail snips of 2-3 mm length were lysed in DirectPCR Lysis Reagent (Viagen Biotech, Las Angeles, CA, USA) containing 0.3 mg/ml proteinase K at 55°C overnight. Lysate was used for PCR analysis with the following primers: 5'CRE (TGCAAGTTGAATAACCG GAAA) and 3'CRE (CTAGAGCCTGTTTTGCACGTTC), and the following program: 36 cycles (40 s at 94°C, 45 s at 57°C, 72 s at 72°C). PCR products were separated by electrophoresis in 1% agarose gel containing 0.05 μl/ml ethidium bromide and visualized with UV light.

Baseline hematological parameters were determined in peripheral blood, collected by retro-orbital puncture into EDTA-coated sample tubes and measured using a HEMAVET 950 veterinary hemocytometer specifically calibrated for mouse blood (Drew Scientific, Oxford, CA, USA).

Wounding. On day 0, 8- to 10-week-old male KO and WT mice were anesthetized by an intraperitoneal injection with Nembutal. The right dorsal flank was shaved and sterilized with alcohol. Full thickness wounds were created with an 8 mm circular, disposable dermal biopsy punch (Miltex, York, PA, USA). The wounds were left open to allow healing through secondary intention. The longest axis of the wound and the axis perpendicular to the longest axis

were measured from cut edge to cut edge using an Absolute Digimatic digital precision caliper instrument (Mitutoyo America Corporation, Aurora, IL, USA). Measurements were taken immediately after wounding and thereafter every other day, until full wound closure (day 15). Both axes were used to calculate the area of the wounds using the formula of an ellipse.

Histology and immunohistochemistry. On day 15 following wounding, animals were sacrificed. An additional group of male HIF 1α KO and WT mice was sacrificed on day 3 following wounding. Tissue specimens of the wounded skin and skin of the non-wounded flank were harvested, fixed in methanol-Carnoy's solution (methanol:chloroform:glacial acetic acid, 6:3:1) and engrossed for histological and immunohistochemical analysis. Tissue sections were deparaffinized, rehydrated, and stained with standard hematoxylin and eosin for general histological analysis.

Immunohistochemical staining of ED2, myeloperoxidase (MPO), transforming growth factor β (TGF-β), and collagen types I and III was performed using methods established and optimized in our laboratory. Tissue sections were deparaffinized and rehydrated. Endogenous peroxidase activity was blocked with 1% H_2O_2 in methanol for 30 min. Non-specific binding was reduced by 10% normal serum (Vector Laboratories, Burlingame, CA, USA) in 3% dry powdered milk in TBS for 30 min. Sections were then incubated with primary antibody for 2 h at room temperature, followed by a 30-min incubation with the appropriate biotinylated secondary antibody (Table I), and avidin-biotin-peroxidase complex (Vector Laboratories) for 30 min. For α-smooth muscle cell (SMC) actin, bound peroxidase was enhanced with biotin-labeled tyramide, followed by streptavidin-bound horseradish peroxidase (TSA Biotin System, PerkinElmer, Shelton, CT, USA). All sections were developed in TBS containing 0.2-0.4 mg/ml 3,3-diaminobenzidine tetrahydro-chloride (DAB) and 0.003% H_2O_2.

Cells positive for ED2 or MPO were identified by color thresholding, using the software package Image-Pro Plus (Media Cybernetics, Silver Spring, MD, USA). The number of immunohistochemically positive cells per 5 fields (×40 objective) was considered a single value for statistical analysis.

In vitro experiments with peritoneal exudate macrophages. In vitro production of IL-1β and NO by peritoneal exudate macrophages after incubation with LPS and/or desferrioxamine (DFX) was measured. Groups of HIF-1α KO and WT mice were injected intraperitoneally with 1 ml 3% thioglycollate. Macrophages were harvested 4 days later by peritoneal lavage and incubated at 2×10^6 cells/ml in RPMI 1640 medium containing 10% FCS, 50 nM 2-mercaptoethanol, 100 U/ml penicillin, and 100 μg/ml streptomycin. After 1 h of incubation at 37°C (95% air, 5% CO_2), nonadherent cells were removed by washing. Macrophages were exposed to 1 μg/ml LPS (*Escherichia coli* 05:B5; Sigma Chemical) and/or 400 μM DFX (Sigma Chemical). After overnight incubation, culture supernatants were collected and assayed for IL-1β by ELISA (R&D Systems) and for NO by the Greiss assay (7).

Statistics. Statistical analysis was performed with the software package NCSS 2000 (NCSS, Kaysville, UT, USA). Differences in wound area were tested with repeated measures ANOVA. Univariate comparisons were performed with the Mann-Whitney *U*-test. *P*-values less than 0.05 were considered statistically significant.

Table I. *Primary and secondary antibodies used for immunohistochemistry.*

Primary antibody	Work dilution	Secondary antibody[a]
Rat anti-ED2 (Serotec, Oxford, UK)	1:100	Rabbit anti-rat IgG
Rabbit anti-MPO (Dako, Glostrup, Denmark)	1:200	Goat anti-rabbit IgG
Pan-specific rabbit anti-TGF-β (R&D, Minneapolis, MN, USA)	1:300	Goat anti-rabbit IgG
Goat anti-collagen I (SouthernBiotech, Birmingham, AL, USA)	1:100	Rabbit anti-goat IgG
Goat anti-collagen III (SouthernBiotech)	1:100	Rabbit anti-goat IgG
Rabbit anti-α-SMC actin (Epitomics, Burlingame, CA, USA)	1:250[b]	Goat anti-rabbit IgG

[a]All secondary antibody were from Vector laboratories and used at a dilutions of 1:400. [b]Signal amplification was used to enhance staining with the rabbit anti-α-SMC actin antibody, as described in the Materials and Methods section.
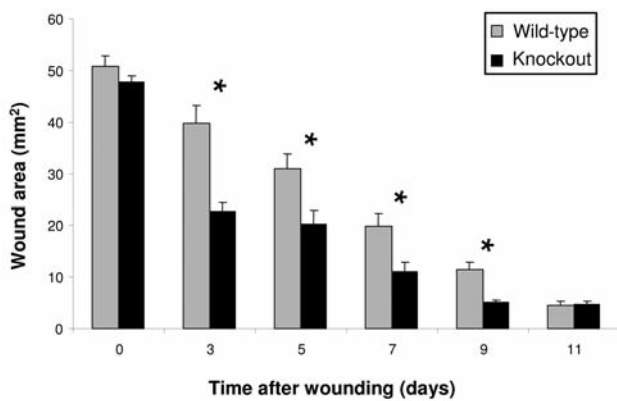

Figure 2. *Secondary intention wound healing in myeloid selective HIF-1α KO and WT mice. Wound area of WT and KO mice, as measured with precision digital calipers immediately after wounding (day 0), and on days 3, 5, 7, 9, and 11 after wounding. The rate of healing during the first 3 days was significantly faster in KO mice than in WT mice (F=39.1, p<0.001). Average, SEM; n=9.*

Figure 3. *Macrophages and neutrophils in granulation tissue from HIF-1α KO and WT mice. Numbers of ED2-positive cells and MPO-positive cells in granulation tissue of WT and KO mice on day 3 after wounding were determined immunohistochemically. No differences were found between WT and KO mice. Average, SEM; n=3-5.*

Table II. *Peripheral blood cell counts in male HIF-1α WT and KO mice (Average±SEM, N=5). None of the differences reached statistical significance.*

	WT	KO
White blood cells ($\times 10^3$/μl)	5.4±0.5	4.9±0.3
Neutrophils ($\times 10^3$/μl)	0.6±0.1	0.7±0.2
Lymphocytes ($\times 10^3$/μl)	3.8±0.1	4.1±0.2
Monocytes ($\times 10^3$/μl)	0.5±0.1	0.5±0.1
Eosinophils ($\times 10^3$/μl)	0.03±0.01	0.01±0.003
Erythrocytes ($\times 10^6$/μl)	11.3±0.1	11.4±0.1
Platelets ($\times 10^6$/μl)	2.1±0.2	2.2±0.2

Results

Wound closure. Peripheral hematological parameters were similar in HIF-1α KO mice and WT controls (Table II).

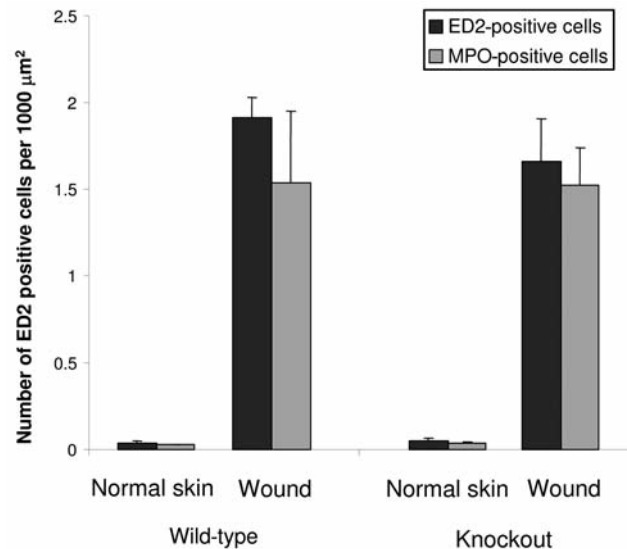Figure 2 shows the wound areas of myeloid-selective HIF-1α KO mice and WT littermates at different time points after wounding. The KO mice exhibited significantly accelerated wound closure when compared with WT mice (F=39.1, p<0.001). The largest difference between the WT and KO mice was observed on day 3. At this time, the average wound area in KO mice was 22.68 mm^2, a 52% reduction from the original wound area, while the average wound area of the WT mice was 38.89 mm^2, a 21% reduction from the original wound area.

On days 13 and 14 wounds were too small for accurate measurement of wound area and were classified as either "fully closed" or "not closed". On day 14, all KO mice had fully closed wounds compared with 78% of WT mice. On day 15, all wounds were fully closed.

Histology and immunohistochemistry. Because the largest difference in wound area between the WT and KO mice was found on day 3, tissue specimens for histological and
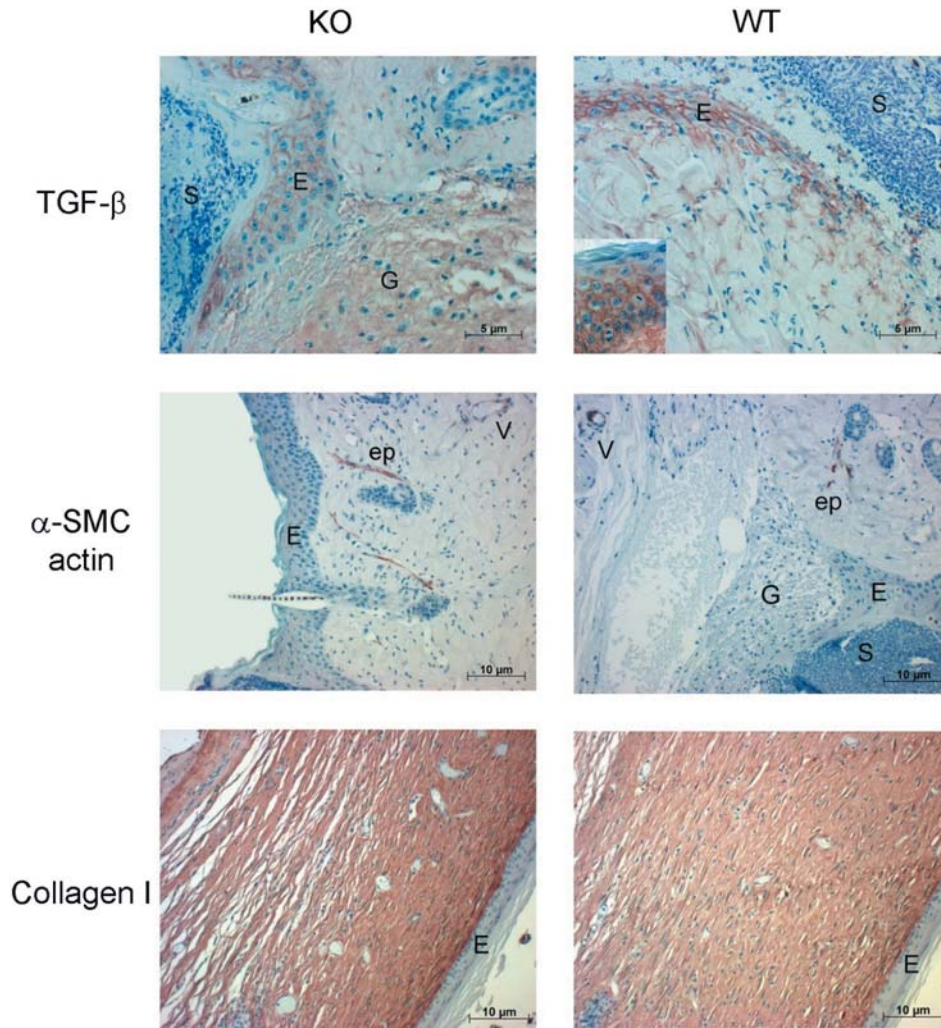
Figure 4. *Immunoreactivity for TGF-β, α-SMC actin, and collagen I in HIF-1α KO and WT mice. Representative images of immunohistochemical stainings of dermal specimens from WT and KO mice. In wounds of day 3, TGF-β was found in granulation tissue and in keratinocytes surrounding the wounds; inset: keratinocytes in mitosis (×100 objective). α-SMC actin was found only in vascular SMC and erector pili. Collagen I immunostaining showed no differences in healed wounds of KO and WT on day 15. E: Epithelial layer, ep: erector pili, G: granulation tissue, S: scab, V: blood vessel.*

immunohistochemical analysis were taken from an additional group of mice on this day.

On day 3, strong TGF-β immunoreactivity was observed in granulation tissue and keratinocytes close to the wound edges (Figure 3). Because activated keratinocytes are known to produce several cytokines and growth factors, including TGF-β (8), keratinocytes positive for TGF-β were counted. Significantly larger numbers of these cells were found surrounding wounded areas of KO mice (503±23) when compared to WT mice (362±14, *p*=0.02). Although α-SMC actin immunoreactivity was found on SMC in the vasculature and in erector pili, no α-SMC actin-positive myofibroblasts were found in wounds in either mouse type at this early time point (Figure 3).

Somewhat surprisingly, WT and KO mice exhibited similar increases in numbers of ED2-positive cells (macrophages) and MPO-positive cells (mainly neutrophils) in wounded areas of (Figure 4).

The healed wounds of WT and KO mice on day 15 showed similar architecture with complete re-epithelization without appreciable signs of scarring (Figure 3). Immunoreactivity for TGF-β was present in the dermis of previously wounded areas, but no longer in the epidermis. On day 15, TGF-β immunoreactivity was similar in WT and KO mice (data not shown).

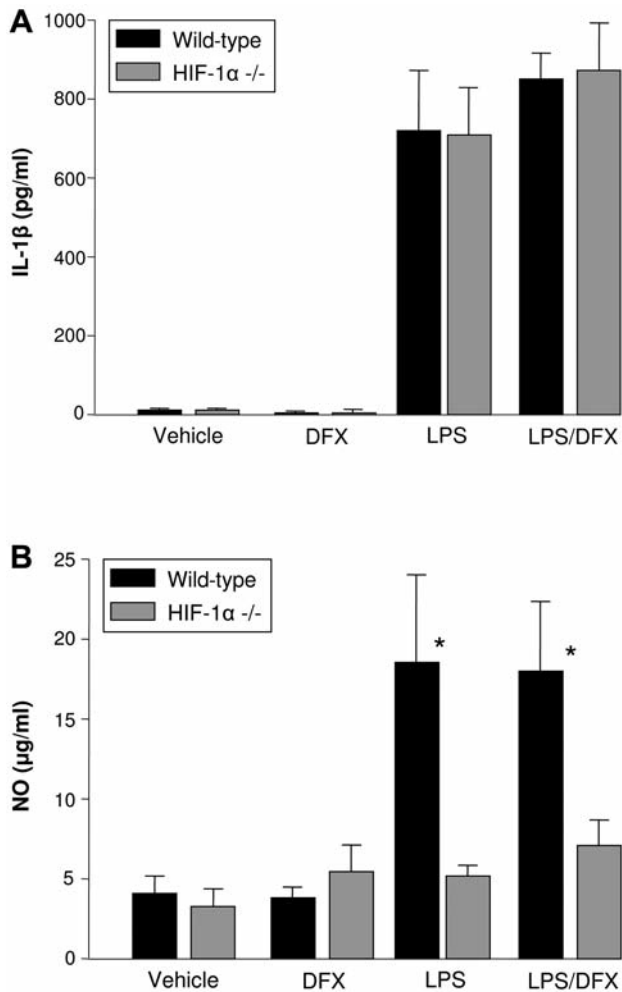*In vitro response of macrophages to LPS and DFX.* LPS induces HIF-1α expression in macrophages (9, 10) and DFX

Figure 5. *Response of peritoneal macrophages from HIF-1α KO and WT mice to lipopolysaccharide (LPS) and desferrioxamine (DFX). Production of IL-1β and NO by peritoneal exudate macrophages was measured after in vitro stimulation with LPS and/or DFX. Panel A: Macrophages from WT and KO mice showed similar up-regulation of IL-1β. Panel B: Macrophages from KO mice failed to increase NO production in response to LPS or a combination of LPS and DFX, resulting in a significant difference between WT and KO macrophages (*p=0.01 and p=0.02, respectively). Average, SD; n=3.*

induces expression of inducible NO synthase in macrophages *via* activation of HIF-1 (11). This study examined the response of HIF-1α KO and WT macrophages to LPS, DFX, or a combination of the two (Figure 5). Macrophages from WT and KO mice showed similar up-regulation of IL-1β in response to LPS or in response to a combination of LPS and DFX. In contrast, production of NO was only induced in macrophages from WT mice, whereas macrophages from KO mice failed to increase NO production in response to these stimuli. DFX alone did not induce a response in WT or KO macrophages.

Discussion

This study, which compared secondary intention healing of full thickness dermal wounds in myeloid-selective HIF-1α KO mice and WT littermates, demonstrates that the deficiency of HIF-1α in myeloid cells is associated with accelerated wound closure during the early phase, while the subsequent healing process occurs at a similar rate. The acceleration of early wound closure, most prominent on day 3, combined with larger numbers of activated keratinocytes without α-SMC actin-positive SMC, suggests that re-epithelialization is the main cause of enhanced wound closure observed in the KO mice.

Neutrophils and macrophages from myeloid-selective HIF-1α KO mice show reduced glycolysis and prominently reduced ATP levels (3). As a result, HIF-1α KO macrophages exhibit reduced *in vitro* aggregation, invasion, motility, reduced bactericidal activity, and reduced production of TNF-α (3) and NO (current study) in response to LPS. On the other hand, HIF-1α KO macrophages do retain phagocytic activity (12). Although macrophages in culture retain their ability to produce IL-1β in response to LPS (current study), *in vivo* production of IL-1β in response to LPS is reduced in myeloid-selective HIF-1α KO mice (10).

Chemical induction of inflammation in myeloid-selective HIF-1α KO mice has been reported to be associated with reduced infiltration of macrophages and neutrophils (3). In contrast, the numbers of these cells were not reduced in wounds in the current study or in models with subcutaneous bacterial infection (12). This suggests that HIF-1α KO myeloid cells, despite being energy-deprived, are able to respond to chemotactic signals and are able to migrate in response to chemotactic signals. Because neutrophils and macrophages were present in normal numbers in wounds of HIF-1α KO mice in our study, the accelerated wound closure was likely caused by functional alterations in these cells.

Neutrophils are one of the earliest inflammatory cell types to infiltrate the wound site. These cells create an inhospitable environment that kills foreign microbes as well as surrounding tissue. Therefore, even though neutrophils may constitute a first barrier to infection, their overall impact on wound healing in the absence of infection may be detrimental. Hence, consistent with our results, neutrophil depletion studies have shown wound closure to be accelerated (13). Although neutrophils derived from myeloid-selective HIF-1α KO mice retain their oxidative burst capacity, they do exhibit reduced granular protease activity (12). Neutrophil-derived proteases, such as elastase, may negatively affect tissue architecture (14, 15). Thus the early gains in wound closure in this study may be a result of an attenuated neutrophil activity that reduces tissue injury.

While neutrophil activity is considered detrimental under certain conditions, macrophages appear to play a mostly beneficial role in wound healing. Depletion of macrophages results in reduced wound healing, likely due to accumulation of debris (16) and injection of macrophages into wound sites promotes wound healing (17). Moreover, whereas wound disruption strength is not affected by neutrophils (13), it is increased after stimulation of macrophages (18). Interestingly, macrophages from myeloid-selective HIF-1α KO mice retain their phagocytic activity (3). It may be speculated that this macrophage function contributed to the accelerated wound closure in myeloid-selective HIF-1α KO mice. The impact of HIF-1α in myeloid cells on wound disruption strength and its possible underlying mechanisms require further investigation.

In conclusion, the early phase of the secondary intention wound healing process appears to be accelerated in myeloid-selective HIF-1α KO mice. This may be related to a deficient NO production response, but further experimentation is required to determine the exact mechanism by which the lack of HIF 1α in myeloid cells regulates wound healing. These findings may have implications for exploring pharmacological modifiers of HIF 1α in the prophylaxis and treatment of abnormal wound healing conditions.

Acknowledgements

References

1 Park JE and Barbul A: Understanding the role of immune regulation in wound healing. Am J Surg *187*: 11S-16S, 2004

2 Martin P and Leibovich SJ: Inflammatory cells during wound repair: the good, the bad and the ugly. Trends Cell Biol *15*: 599-607, 2005

3 Cramer T, Yamanishi Y, Clausen BE, Forster I, Pawlinski R, Mackman N, Haase VH, Jaenisch R, Corr M, Nizet V, Firestein GS, Gerber HP, Ferrara N and Johnson RS: HIF-1alpha is essential for myeloid cell-mediated inflammation. Cell *112*: 645-657, 2003.

4 Ke Q and Costa M: Hypoxia-inducible factor-1 (HIF-1). MolPharmacol *70*: 1469-1480, 2006.

5 Albina JE and Reichner JS: Oxygen and the regulation of gene expression in wounds. Wound Repair Regen *11*: 445-451, 2003.

6 Clausen BE, Burkhardt C, Reith W, Renkawitz R and Forster I: Conditional gene targeting in macrophages and granulocytes using LysMcre mice. Transgenic Res *8*: 265-277, 1999.

7 Ding AH, Nathan CF and Struehr DJ: Release of reactive oxygen intermediates from mouse peritoneal macrophages. J Immunol *141*: 2407-2412, 1988.

8 Schmid P, Cox D, Bilbe G, McMaster G, Morrison C, Stahelin H, Luscher N and Seiler W: TGF-beta s and TGF-beta type II receptor in human epidermis: differential expression in acute and chronic skin wounds. J Pathol *171*: 191-197, 1993.

9 Blouin CC, Page EL, Soucy GM and Richard DE: Hypoxic gene activation by lipopolysaccharide in macrophages: implication of hypoxia-inducible factor 1alpha. Blood *103*: 1124-1130, 2004.

10 Peyssonnaux C, Cejudo-Martin P, Doedens A, Zinkernagel AS, Johnson RS and Nizet V: Cutting edge: Essential role of hypoxia inducible factor-1alpha in development of lipopolysaccharide-induced sepsis. J Immunol *178*: 7516-7519, 2007.

11 Melillo G, Taylor LS, Brooks A, Musso T, Cox GW and Varesio L: Functional requirement of the hypoxia-responsive element in the activation of the inducible nitric oxide synthase promoter by the iron chelator desferrioxamine. J Biol Chem *272*: 12236-12243, 1997.

12 Peyssonnaux C, Datta V, Cramer T, Doedens A, Theodorakis EA, Gallo RL, Hurtado-Ziola N, Nizet V and Johnson RS: HIF-1alpha expression regulates the bactericidal capacity of phagocytes. J Clin Invest *115*: 1806-1815, 2005.

13 Dovi JV, He LK and DiPietro LA: Accelerated wound closure in neutrophil-depleted mice. J Leukoc Biol *73*: 448-455, 2003.

14 Dovi JV, Szpaderska AM and DiPietro LA: Neutrophil function in the healing wound: adding insult to injury? Thromb Haemost *92*: 275-280, 2004.

15 Briggaman RA, Schechter NM, Fraki J and Lazarus GS: Degradation of the epidermal-dermal junction by proteolytic enzymes from human skin and human polymorphonuclear leukocytes. J Exp Med *160*: 1027-1042, 1984.

16 Leibovich SJ and Ross R: The role of the macrophage in wound repair. A study with hydrocortisone and antimacrophage serum. Am J Pathol *78*: 71-100, 1975.

17 Danon D, Kowatch MA and Roth GS: Promotion of wound repair in old mice by local injection of macrophages. Proc Natl Acad Sci USA *86*: 2018-2020, 1989.

18 Browder W, Williams D, Lucore P, Pretus H, Jones E and McNamee R: Effect of enhanced macrophage function on early wound healing. Surgery *104*: 224-230, 1988.